

Synoptic Evaluation of Scale-Dependent Metrics for Hydrographic Line Feature Geometry

Lawrence V. Stanislawski¹, Barbara P. Battenfield², Paulo Raposo³, M. Cameron¹, Jeff Falgout⁴

¹ U.S. Geological Survey, Center of Excellence for Geospatial Information Science, 1400 Independence Road, Rolla MO 65401
Email: lstan@usgs.gov

²University of Colorado-Boulder, Boulder, CO 80309-0260
Email: babs@colorado.edu

³Department of Geography, Pennsylvania State University, University Park PA 16802
Email: paulo.raposo@psu.edu

⁴ U.S. Geological Survey, Core Science Analysis, Synthesis, and Libraries, Denver Federal Center, Denver CO 80225
Email: jfalgout@usgs.gov

Disclaimer: Any use of trade, firm, or product names is for descriptive purposes only and does not imply endorsement by the U.S. Government.

1. Introduction

Methods of acquisition and feature simplification for vector feature data impact cartographic representations and scientific investigations of these data, and are therefore important considerations for geographic information science (Haunert and Sester 2008). After initial collection, linear features may be simplified to reduce excessive detail or to furnish a reduced-scale version of the features through cartographic generalization (Regnauld and McMaster 2008, Stanislawski et al. 2014). A variety of algorithms exist to simplify linear cartographic features, and all of the methods affect the positional accuracy of the features (Shahriari and Tao 2002, Regnauld and McMaster 2008, Stanislawski et al. 2012). In general, simplification operations are controlled by one or more tolerance parameters that limit the amount of positional change the operation can make to features. Using a single tolerance value can have varying levels of positional change on features; depending on local shape, texture, or geometric characteristics of the original features (McMaster and Shea 1992, Shahriari and Tao 2002, Battenfield et al. 2010). Consequently, numerous researchers have advocated calibration of simplification parameters to control quantifiable properties of resulting changes to the features (Li and Openshaw 1990, Raposo 2013, Tobler 1988, Veregin 2000, and Battenfield, 1986, 1989).

This research identifies relations between local topographic conditions and geometric characteristics of linear features that are available in the National Hydrography Dataset (NHD). The NHD is a comprehensive vector dataset of surface

water features within the United States that is maintained by the U.S. Geological Survey (USGS). In this paper, geometric characteristics of cartographic representations for natural stream and river features are summarized for subbasin watersheds within entire regions of the conterminous United States and compared to topographic metrics. A concurrent processing workflow is implemented using a Linux high-performance computing cluster to simultaneously process multiple subbasins, and thereby complete the work in a fraction of the time required for a single-process environment. In addition, similar metrics are generated for several levels of simplification of the hydrographic features to quantify the effects of simplification over the various landscape conditions.

Objectives of this exploratory investigation are to quantify geometric characteristics of linear hydrographic features over the various terrain conditions within the conterminous United States and thereby illuminate relations between stream geomorphological conditions and cartographic representation. The synoptic view of these characteristics over regional watersheds that is afforded through concurrent processing, in conjunction with terrain conditions, may reveal patterns for classifying cartographic stream features into stream geomorphological classes. Furthermore, the synoptic measurement of the amount of change in geometric characteristics caused by the several levels of simplification can enable estimation of tolerance values that appropriately control simplification-induced geometric change of the cartographic features within the various geomorphological classes in the country. Hence, these empirically derived rules or relations could help generate multiscale-representations of features through automated generalization that adequately maintain surface drainage variations and patterns reflective of the natural stream geomorphological conditions across the country.

2. Methods

This paper extends the preliminary work by Stanislawski et al. (2012) in which ten subbasins of NHD stream linear features from three terrain slope conditions of the conterminous United States were stratified into three stream density classes. Geometric characteristics of the original and simplified features in the subbasin density classes were assessed for five simplification tolerances. Stanislawski et al. (2012) noted a consistent positive relation between the displacement and segment length metrics with the Bend-Simplify (Wang and Muller 1998) tolerance values that were applied to the features.

Features in the NHD flowline network include streams, rivers, canals, ditches, pipelines, artificial paths, and connectors. Artificial paths are synthetic features that connect network features where interrupted by polygonal waterbodies, and connectors are added to the network in places where surface flow is known to exist but no feature was included in the source material (U. S. Geological Survey, 2000). In this research, the natural flowline features from a subbasin, having stream/river feature type, are subdivided into density classes using density class breaks of less than 1.0, between 1.0 and less than 2.5, and greater than 2.5 kilometers per square kilometer (km/km^2) for the low-, medium-, and high-density partitions, respectively. An example set of density partitions for the Upper Connecticut River is shown in Figure 1. Class values in the figure represent average density values generated for this particular subbasin. Line-density partitions are generated through a raster-based approach with a minimum mapping unit of 15 square kilometers (km^2) (Stanislawski and Bittenfield, 2011). Stream/river features are simplified using the Bend-Simplify algorithm (Wang and

Muller 1998) with seven tolerance values of 15, 25, 50, 100, 200, 300, and 500 meters. Computations are performed with custom-developed Python geoprocessing scripts using Esri's ArcGIS® Desktop and Server tools and functions.

Subbasin datasets are processed on a distributed memory high performance Linux cluster. Data processing resources on the cluster are controlled by a job scheduler and resource manager. Two different high performance computing environments are available for processing. The first is a traditional distributed memory compute cluster of International Business Machines (IBM®) X3650 machines, and the second high performance computing environment is a UV 2000 shared memory system from Silicon Graphics, Inc. (SGI®). This architecture allows many datasets to be processed simultaneously, which enables analysis of data at regional, national, and continental scales.

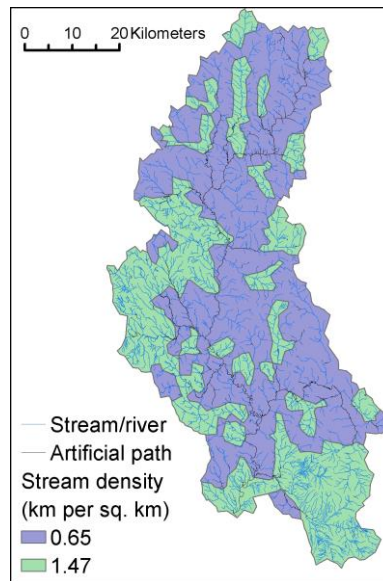


Figure 1. Density partitions generated for Upper Connecticut River subbasin (01080101). Density classification is described in the text.

2.1 All-feature Metrics

Metrics that can be computed for all features in a subbasin are referred to as all-feature metrics. Metric values are computed for each feature having stream/river feature type, where a feature represents a confluence-to-confluence segment of a stream or river. All-feature metrics are separately averaged for original and simplified features within each density partition. These metrics are computed for all subbasins in Regions 1 and 7 (Figure 2). Average values are transferred to associated density partition polygons for each subbasin, and subsequently the density partitions are appended for an entire region to ease visual analysis of the data. All-feature metrics include sinuosity, segment length, error variance, and absolute angularity.

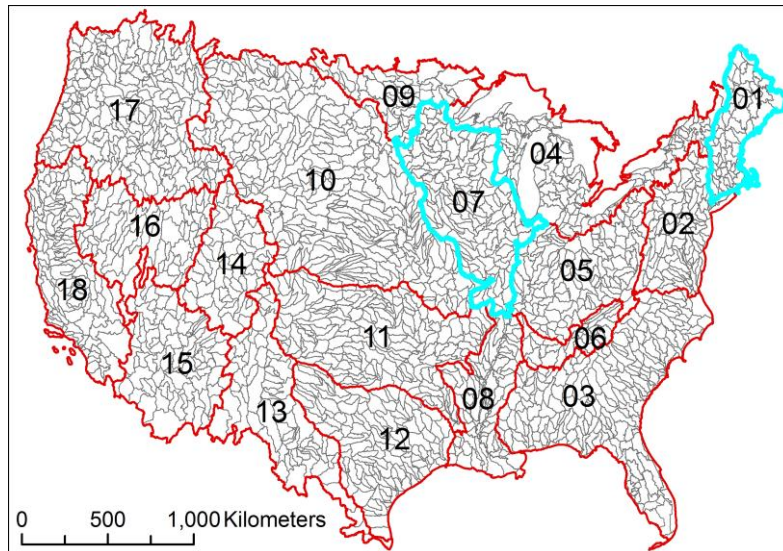


Figure 2. National Hydrography Dataset (NHD) subregion watersheds in the conterminous United States displayed with red boundaries. Initial test regions 01 and 07 are outlined with cyan boundaries. Subbasin watershed boundaries are displayed with gray boundaries.

Average sinuosity. The sinuosity of a line feature is defined as the total length of all polyline line segments divided by the distance between the polyline endpoints. Average sinuosity is computed by averaging the sinuosity of all features in a density class.

Mean of average segment length per feature. Average segment length per feature is the total length of a feature divided by the number of line segments in the feature. The mean value is the mean of all average segment lengths per feature in a density class.

Average error variance. Error variance of a feature is the sum of the perpendicular distances of each non-endpoint vertex in the feature to the anchor line of the feature, where the anchor line is the line between the two end points (Buttenfield 1986, Shariari et al. 2002). Average error variance for a density class is computed from all features in a density class of a subbasin.

Average absolute angularity. Absolute angularity of a feature is the sum of absolute value of direction changes from one segment to the next in a feature divided by the number of direction changes in the feature (Buttenfield 1991, Bernhardt 1992, Tsoulos and Skopeliti 2000). The values are averaged for all features in each density class of each subbasin.

All-feature metrics averaged over the subbasin density partitions for Regions 1 and 7 are compared to average channel density values and average stream morphological characteristics of the terrain within each density partition. Stream morphological characteristics include soil permeability, rock depth, slope, runoff and vegetative cover. Soil permeability in millimeters per hour (mm/hour) and rock depth in mm are estimated from a 1-kilometer (km) resolution raster dataset compiled from the State Soil Geographic (STATSGO) Database (U.S. Department of Agriculture 1993). Average slope for each partition is estimated from a 5-km resolution raster dataset

compiled from USGS 1:250,000-scale, 3-arc-second digital elevation models. Average runoff values are computed from a 5-km cell runoff model that estimates mean annual runoff from 1951 to 2000 through a water balance model which only considers effects of precipitation and temperature (Wolock and McCabe 1999, McCabe and Markstrom 2007, McCabe and Wolock 2008). Vegetative cover is estimated from an 18-year average of mean annual Normalized Difference Vegetation Index (NDVI) values from 1990 to 2010, skipping 1992, 1993, and 1994 because of errors in those datasets. Mean annual NDVI values are produced from Advanced Very High Resolution Radiometer data. Possible relations between all-feature metrics and the stream morphological characteristics are evaluated through regression equations and associated R^2 values. The R^2 value, or *coefficient of multiple determination*, represents the proportion of the variation in the dependent variable that is explained by the regression model (McClave and Dietrich 1979). Data patterns of the channel characteristics with the density partitions are also visually compared with patterns in the raster datasets representing the stream morphology conditions.

2.2 Displacement Metrics

Displacement metrics computed for this study include maximum Hausdorff distance and average areal displacement. Displacement metrics compare original features with simplified features to estimate the amount of coordinate shift and elimination caused by the simplification process. Displacement computations using Esri ArcGIS® geoprocessing functions are very time-consuming. To reduce processing time, displacement metrics are computed for a 5-percent sample of features in any density class having more than 1,000 features; otherwise all features are used. Sample features are selected by sorted length to preserve a length distribution similar to the distribution of all features in the associated density class. Displacement metrics are only computed for 30 subbasins that are distributed over the conterminous United States in different slope and runoff categories (Figure 3).

Maximum Hausdorff distance. The Hausdorff distance between two linear features can be defined as the largest minimum distance between any point on one feature to any point on the other (Hangouët, 1995; Rucklidge, 1996; Nutanong, 2011). This is an important measure to compare along with areal displacement because a feature could have a large displacement area without the lines deviating significantly from their source features. A Hausdorff distance is computed between the original geometry and a simplified version of the feature's geometry. A maximum Hausdorff distance for each density class in a subbasin is determined from the Hausdorff distances for the set of features in each density class. Preliminary results suggest that maximum Hausdorff distances for all subbasins in all density classes and tolerance values range from about 0 to 660 m.

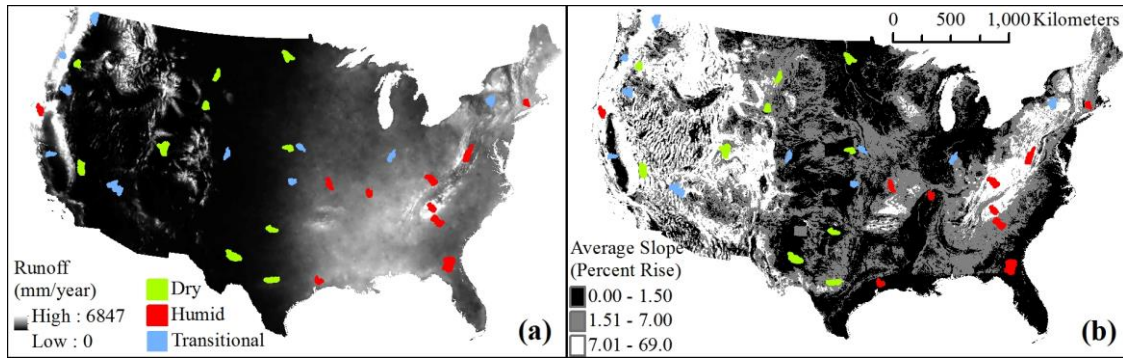


Figure 3. Thirty subbasins distributed over the conterminous United States in three slope and two runoff categories, and one transitional category. Dry conditions experience less than 140 mm/year runoff, while humid regions experience more runoff. Transitional subbasins are in conditions that span more than one slope or runoff category.

Similar to other displacement metrics, the Hausdorff distance computation is also computationally intensive, as it requires checking the distance from every point in a source feature to all points in the generalized version of the feature is computationally intensive. Consequently, an alternate, approximate method for computing Hausdorff distance was used that constructs the minimum bounding rectangle (MBR) around each displacement polygon for a feature. The maximum vector displacement (MVD) for a polygon is determined by comparing the length and width of the MBR with the length of the intersection of the simplified line with the displacement polygon. If the difference between the MBR width and the intersection length is greater than the difference of the MBR length and the intersection length, then the MVD for the polygon is estimated as the width of the MBR, otherwise the MVD is the length of the MBR. The Hausdorff distance for a feature is the maximum MVD for all displacement polygons of the feature.

Average areal displacement. The areal displacement for a linear feature is the sum of the area of all displacement polygons created between the original and simplified line feature divided by the length of the original line (White 1985, McMaster 1986). Average areal displacement is computed for each density class in a subbasin as the average of the areal displacements for all features in the density class.

3. Preliminary Results and Discussion

3.1 All-feature Metrics

R^2 values resulting from best-fitting regression equations predicting an all-feature stream metric from a stream morphology characteristic are summarized in Table 1. Average sinuosity and error variance values of stream features for density partitions in Regions 1 and 7 appear weakly related with average stream morphology characteristics; whereas average absolute angularity and average segment length values do not appear associated with any of the estimated stream morphology conditions. Sinuosity appears primarily related to runoff ($0.53 R^2$), but is also partially affected by slope, permeability and rock depth. Error variance appears mostly related to permeability ($0.61 R^2$) and is more weakly related with runoff, channel density, and

rock depth. However, lack of or weak relations may be caused by the coarse resolution (1 km and 5 km cell sizes) raster datasets that are used to represent the stream morphology conditions. Morphology estimates based from finer resolution data may yield stronger correlations.

Table 1. R^2 values (rounded to two decimal places) from regression equations that best predict the stream morphology characteristic from the 1:24,000-scale stream feature metric. Regression equations are estimated from average values for each subbasin density partition within National Hydrography Dataset (NHD) regions 1 and 7. Values greater than 0.3 are shaded. NDVI, Normalized Difference Vegetation Index.

Feature Metrics	Sinuosity	Error Variance	Absolute Angularity	Segment Length
Morphology Characteristic				
Slope	0.16	0.07	0.00	0.01
Channel Density	0.03	0.30	0.00	0.00
NDVI	0.02	0.04	0.02	0.07
Permeability	0.13	0.61	0.02	0.03
Rock Depth	0.15	0.15	0.01	0.00
Runoff	0.53	0.40	0.00	0.01

Average sinuosity of streams within the subbasin density partitions is inversely related to local landscape runoff over Regions 1 and 7, and this relation persists after stream features are simplified through the Bend-Simplify algorithm with a 500-m tolerance (Figure 4). The spatial distribution of sinuosity and runoff values (Figure 5) portrays this inverse relation over the measured landscapes in the north-eastern section of the conterminous United States.

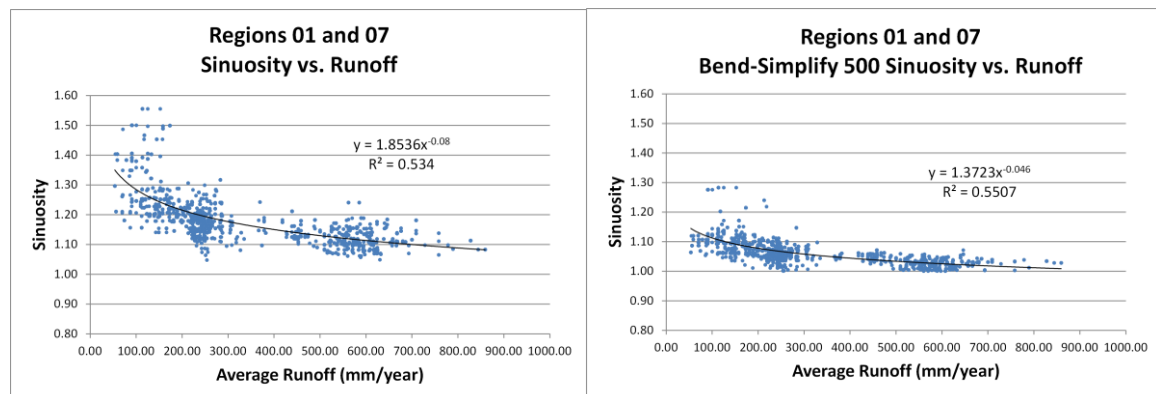


Figure 4. Plot of average sinuosity compared to average mean annual runoff for the subbasin density partitions in Regions 1 and 7 of the National Hydrography Dataset. Average sinuosity values are shown for 1:24,000-scale stream features before (left) and after (right) simplification using a 500-m tolerance with the Bend-Simplify algorithm (Wang and Muller 1998). Regression equations and R^2 values are included.

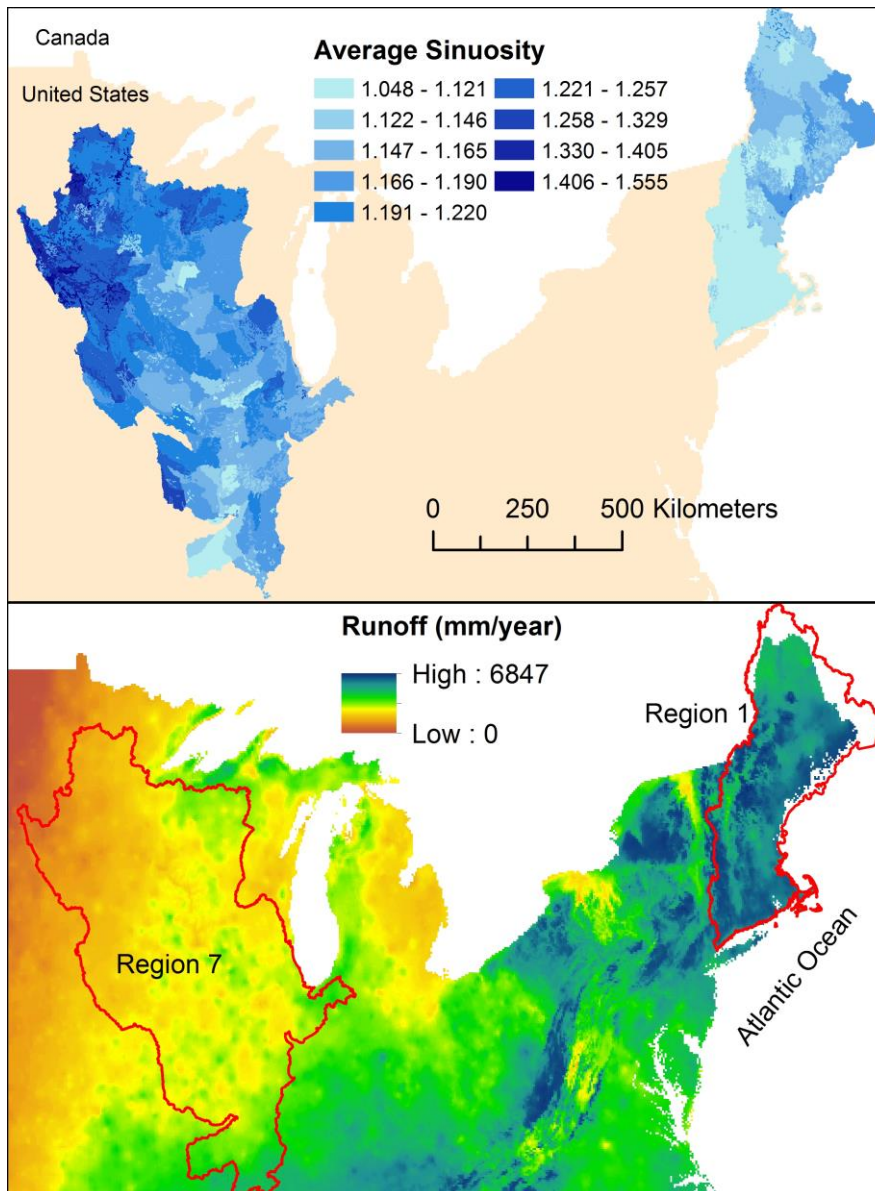


Figure 5. Spatial distribution of average sinuosity values (top) of 1:24,000-scale stream features within density partitions for subbasin within Regions 1 and 7 of the National Hydrography Dataset. The spatial pattern of mean annual runoff values (bottom) estimated for years between 1951-2000 for 5-km cells from (McCabe and Wolock 2008) demonstrates an inverse relation with stream sinuosity. Runoff displayed through histogram equalization contrast stretch.

Schumm (1963) suggests that channel sediment load influences channel stability, shape, and sinuosity, and he proposes a river channel classification based on channel stability and the primary mode of sediment transport. The type and amount of sediment load depends on the local landscape. Later, Schumm and Khan (1972), and Schumm (1973) add that sediment load is regulated by valley slope, and that critical thresholds of sediment load and slope alter a channel's pattern, which cause variations in channel sinuosity over the course of the river channel. A general outline for changes in sinuosity over the course of a typical river is described as follows. Sinuosity is low in higher-slope cutting headwater channels. Sinuosity increases somewhat as river channels flow downhill picking up sediment and moving to lower slope areas. At a

phase where some sediment load is deposited, an alluvial fan and or braids may form that have lower sinuosity than immediate uphill sections of the river system. Over time, sediment deposits accumulate in an outwash plain that has relatively low erosion resistance, and, where the slope of the plain is steep enough, a meandering channel having a maximum sinuosity for the river system will form over the flood plain. Even further downhill, sediment loads dissipate as does slope, and channels become straighter. This scenario explains channel sinuosity variations within a local watershed. However, as seen in Figure 5, the sinuosity levels in Regions 1 and 7 vary between watersheds having different geology, terrain and climate conditions that control sediment capacity, erosion resistance, and slope.

Lazarus and Constantine (2013) offer a generic theory for channel sinuosity. They propose and demonstrate through a mathematical model that sinuosity is directly related to flow resistance relative to mean landscape slope, where flow resistance is affected by landscape roughness attributable to topography and vegetation density. Under this theory, landscapes dominated with high flow resistance compared to slope will have higher channel sinuosity values than landscapes where slope is a more dominant factor. Although results are preliminary, this theory may partially explain the inverse relation between runoff and sinuosity seen in Figure 5. The slope dominated conditions in Region 1 where runoff is high show lower sinuosity values than in Region 7 where average slope values and runoff values are lower. Further evaluation for the other regions of the conterminous United States is needed to validate and refine these relations.

Average error variance values of streams within the subbasin density partitions is inversely related to local permeability values in Region 1 and 7, but few partitions have relatively high permeability values in these regions (Figure 6). As with runoff, simplification with a 500 tolerance does not eliminate the relation of error variance with permeability (Figure 6). The spatial distributions of stream feature error variance and soil permeability are displayed in Figure 7. Permeability affects surface water runoff and likewise other interactions exist among the stream geomorphological factors and the impacts on stream channel geometry characteristics. Further analysis over the remainder of the conterminous United States should validate relations demonstrated here and simplify analysis of the inter-relations among these data.

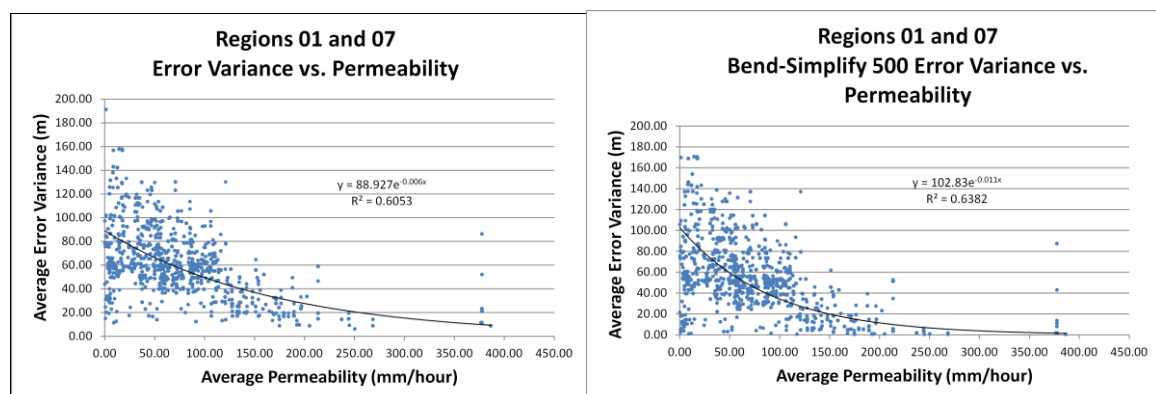


Figure 6. Plot of average error variance compared to average permeability for the subbasin density partitions in Regions 1 and 7 of the National Hydrography Dataset.

Average error variance values are shown for 1:24,000-scale stream features before (left) and after (right) simplification using a 500-m tolerance with the Bend-Simplify algorithm (Wang and Muller 1998). Regression equations and R^2 values are included.

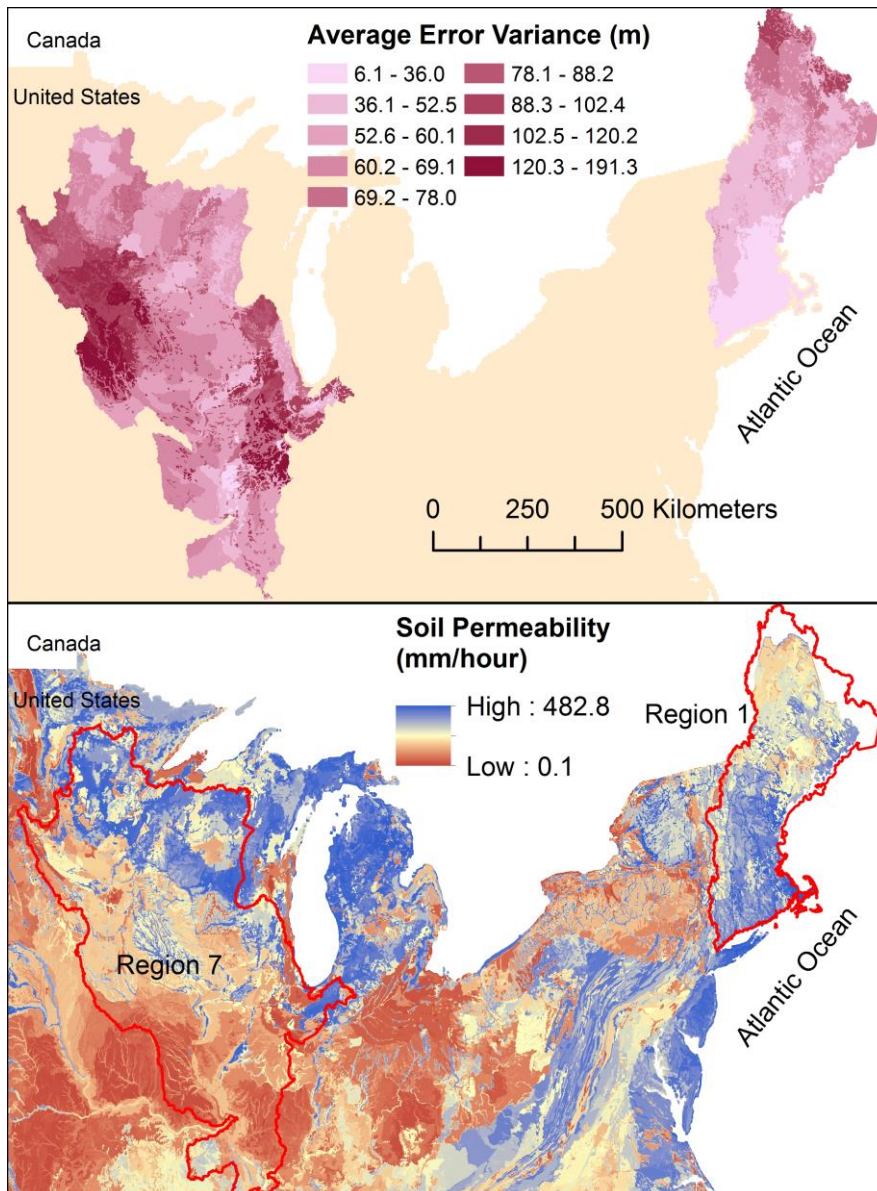


Figure 7. Spatial distribution of average error variance values (top) of 1:24,000-scale stream features within density partitions for subbasin within Regions 1 and 7 of the National Hydrography Dataset. The spatial pattern of permeability (bottom) in millimeters per hour (mm/hour) estimated from a 1-kilometer (km) resolution raster dataset compiled from the State Soil Geographic (STATSGO) Database (U.S. Department of Agriculture 1993) demonstrates an inverse relation with the error variance of the digital stream features. Permeability displayed through histogram equalization contrast stretch.

3.2 Effect of Simplification

Some preliminary results presented here demonstrate the variability of the metrics in different geographic conditions and the magnitude of change caused by different Bend-Simplify tolerance values. Preliminary results of average sinuosity for three subbasins are presented in Figure 8. An inverse relationship exists between average sinuosity and tolerance values, with the most change in average sinuosity being exhibited in the

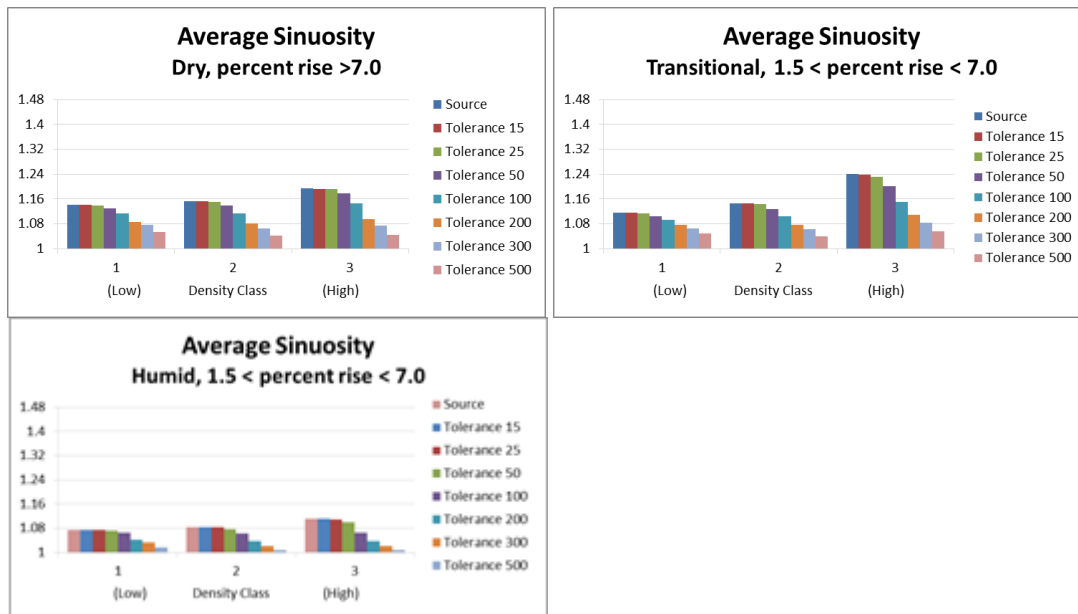


Figure 8. Average sinuosity values for original source stream/river features and simplified features from seven Bend-Simplify tolerance values. Feature sinuosity values are averaged for each density class for dry Utah subbasin 14060005 with average slope greater than 7.0 percent rise (upper left), transitional Oregon subbasin 18010202 with average slope between 1.5 and 7.0 percent rise (upper right), and humid Connecticut subbasin 01100002 with average slope between 1.5 and 7.0 percent rise (lower left).

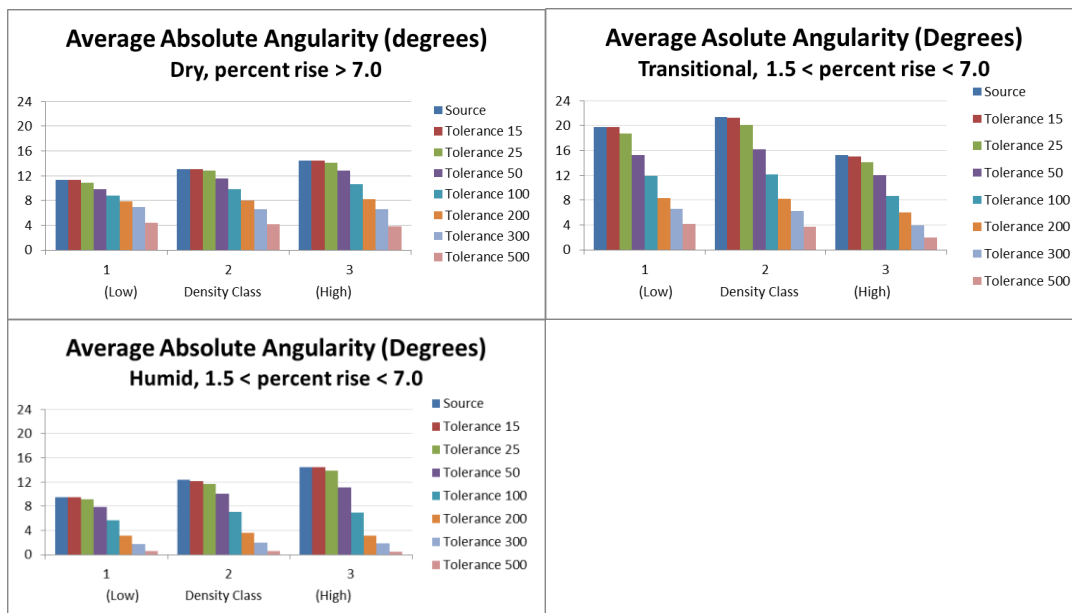


Figure 9. Average absolute angularity values for original source stream/river features and simplified features from seven Bend-Simplify tolerance values. Absolute angularity values are averaged for each density class for dry Utah subbasin 14060005 with average slope greater than 7.0 percent rise (upper left), transitional Oregon subbasin 18010202 with average slope between 1.5 and 7.0 percent rise (upper right), and humid Connecticut subbasin 01100002 with average slope between 1.5 and 7.0 percent rise (lower left).

highest density classes for these three subbasins. The inverse relation of sinuosity with simplification tolerance is expected because complex linear features typically become straighter with more simplification.

In contrast, Figure 9 shows that average absolute angularity is affected slightly differently in the three subbasins. Again, an inverse relationship exists between angularity and tolerance for all three subbasins, and the most change with tolerance within a subbasin is seen in the high density strata for the dry and humid subbasins. However, the least amount of change in angularity with tolerance is exhibited in the high density class for the transitional subbasin. Furthermore, the transitional subbasin displays a more pronounced decrease in angularity with tolerance across density strata, with higher source angularities than exhibited by the dry and humid subbasins.

4. Summary

This research identifies general patterns in cartographic representations of stream features and relationships with stream geomorphological characteristics of local geography. Preliminary results relate two geometric characteristics with local stream density. As demonstrated by these results, geometric characteristics of stream features, along with changes caused by simplification, can vary in different ways depending on geographic conditions. The synoptic computation and visual display of these characteristic, along with geographic conditions, enables exploration and identification of common patterns of these data. Additional metrics and geographic characteristics will be shown at the workshop.

Results from this research will permit examination of patterns and relationships between feature characteristics and geographic conditions. This will allow development of control for simplification tolerance that maintains consistent changes to feature geometries through all geomorphological conditions in the conterminous United States across a range of scales.

5. References

- Bernhardt M C, 1992, Quantitative characterization of cartographic lines for generalization. Report No. 425, Department of Geodetic Science and Surveying, The Ohio State University, Columbus, Ohio, 142p.
- Buttenfield B P, 1986, Digital definitions of scale-dependent line structure. *AutoCarto* London Conference, London, England, September 14-19, pp. 497-506.
- Buttenfield B P, 1989, Scale-dependence and self-similarity in cartographic lines. *Cartographica*, 26(1): 79-100.
- Buttenfield B, 1991, A rule for describing line feature geometry. 150-171 pp. in Buttenfield B, and McMaster R, (eds.), *Map Generalization*, Longman Scientific, Harlow, Essex, U.K..
- Buttenfield B P, Stanislawski, L V, and Brewer C A, 2010, Multiscale representations of water: Tailoring generalization sequences to specific physiographic regimes. *Proceedings, 6th International Conference on Geographic Information Science*, Zurich, Switzerland, September 14-17, 6p.
- Hangouët J F, 1995, Computation of the Hausdorff distance between plane vector polylines. *AutoCarto12 Conference*, Charlotte, North Carolina.

- Haunert J H, and Sester M, 2008, Assuring logical consistency and semantic accuracy in map generalization. *Photogrammetry – Remote Sensing – Geoinformation (PFG)*, 2008(3): 165-173.
- Lazarus E D, and Constantine J A, 2013, Generic theory for channel sinuosity, *Proceedings National Academy of Sciences* 110(21): 8447-8452.
- Li Z, and Openshaw S, 1990, A natural principle of objective generalization of digital map data and other spatial data. *RRL Research Report: CURDS*, University of Newcastle upon Tyne.
- McCabe G J, and Markstrom S L, 2007, A monthly water-balance model driven by a graphical user interface. U.S. Geological Survey, Open-File Report 2007-1088, 6pp.
- McCabe G J, and Wolock, D M, 2008, Joint variability of global runoff and global sea surface temperatures. *Journal of Hydrometeorology* 9: 816–824. doi:10.1175/2008JHM943.1
- McClave J T, and Dietrich F H II, 1979, *Statistics*. Dellen Publishing Company, San Francisco CA, 681p.
- McMaster R B, 1986, A statistical analysis of mathematical measure for linear simplification. *The American Cartographer*, 13(2): 103-116.
- McMaster R B, and Shea K S, 1992, *Generalization in Digital Cartography*. Association of American Geographers, Washington DC, 134p.
- Nutanong S, Jacox E H, and Samet H, 2011, An incremental Hausdorff distance calculation algorithm. *37th International Conference on Very Large Data Bases*, Seattle, Washington, August 29-September 3.
- Raposo, P, 2013, Scale-specific automated line simplification by vertex clustering on a hexagonal tessellation. *Cartography and Geographic Information Science*, 40(5): 427-443.
- Regnauld N, and McMaster R B, 2007, A synoptic view of generalization operators.al networks. Chapter 3:37-66 in Mackaness W A, Ruas A, and Sarjakoski L T (eds.), *Generalization of Geographic Information: Cartographic Modelling and Applications*. Elsevier for International Cartographic Association, 370p.
- Rucklidge W, 1996, *Efficient Visual Recognition Using the Hausdorff Distance*. Berlin: Springer Verlag.
- Schumm S A, 1963, A tentative classification of alluvial river channels: an examination of similarities and differences among some Great Plains rivers. *U.S. Geological Survey Circular 477*, Washington D.C., 10p.
- Schumm S A, 1973, Geomorphic thresholds and complex response of drainage systems. *Fluvial Geomorphology* 6:69-85.
- Schumm S A, and Khan H R, 1972, Experimental study of channel patterns. *Geological Society of America Bulletin* 83: 1755-1770.
- Shahriari N, and Tao V, 2002, Minimising positional errors in line simplification using adaptive tolerance values. *ISPRS Commission IV, Symposium on Geospatial Theory, Processing and Applications*, Ottawa, Canada, July 9-12.
- Stanislawski L V, and Battenfield B P 2011, A raster alternative for partitioning line densities to support automated cartographic generalization. *25th International Cartography Conference*, Paris, July 3-8.
- Stanislawski L V, Battenfield B P, Bereuter P, Savino, S, and Brewer C A, 2015, Generalization operators. Chapter 6:157-195, in Burghardt D, Duchene C, and Mackaness W A (eds.), *Abstracting Information in a Data Rich World: Methodologies and Applications of Map Generalization*. Springer, Berlin, 407pp.

- Stanislawski L V, Doumbouya A T, Miller-Corbett C D, Battenfield B P, and Arundel S T, 2012, Scaling stream densities for hydrologic generalization. *Proceedings, 7th International Conference on Geographic Information Science*, Columbus, Ohio, September 18-21, 6 p.
- Stanislawski, L V, Raposo P, Howard M, and Battenfield B P, 2012, Automated metric assessment of line simplification in humid landscapes, *AutoCarto 2012 Proceedings*, Columbus, Ohio, September 16-18, 14p.
- Tobler W R, 1988, Resolution, resampling, and all that. 129-137pp in Mounsey H, and Tomlinson R F, (eds.), *Building Databases for Global Science: Proceedings of 1st Meeting of the International Geographical Union Global Database Planning Project*, Taylor and Francis, Hampshire, U.K.
- Tsoulos L, and Skopeliti A, 2000, Assessment of data acquisition error for linear features. *International Archives of Photogrammetry and Remote Sensing*, 33: 1087-1091.
- U.S. Department of Agriculture, 1993, State soil geographic data base (STATSGO): Data users guide. U.S. Department of Agriculture Miscellaneous Publication Number 1492, Washington DC.
- Veregin H, 2000, Quantifying positional error induced by line simplification. *International Journal of Geographical Information Science*, 14(2): 113-130.
- Wang Z, and Muller J C, 1998, Line generalization based on analysis of shape characteristics. *Cartography and Geographic Information Science*, 25(1): 3-15.
- White E R, 1985, Assessment of line-generalization algorithms using characteristic points. *The American Cartographer*, 12(1): 17-27.
- Wolock D M, and McCabe G J, 1999, Estimates of runoff using water-balance and atmospheric general circulation models.” *Journal of the American Water Resources Association* 35 (6): 1341–1350. doi:10.1111/jawr.1999.35.issue-6.